AD-A056 975 TENNESSEE UNIV KNOXVILLE ULTRASONICS LAB F/G 20/1
RAYLEIGH-LIKE REFLECTION OF ULTRASONIC WAVES AT A LIQUID-SOLID --ETC(U)
JUN 78 D A MCCATHERN N00014-76-C-0177
UNCLASSIFIED TR-16 NL

1 OF 1
AD A056 975

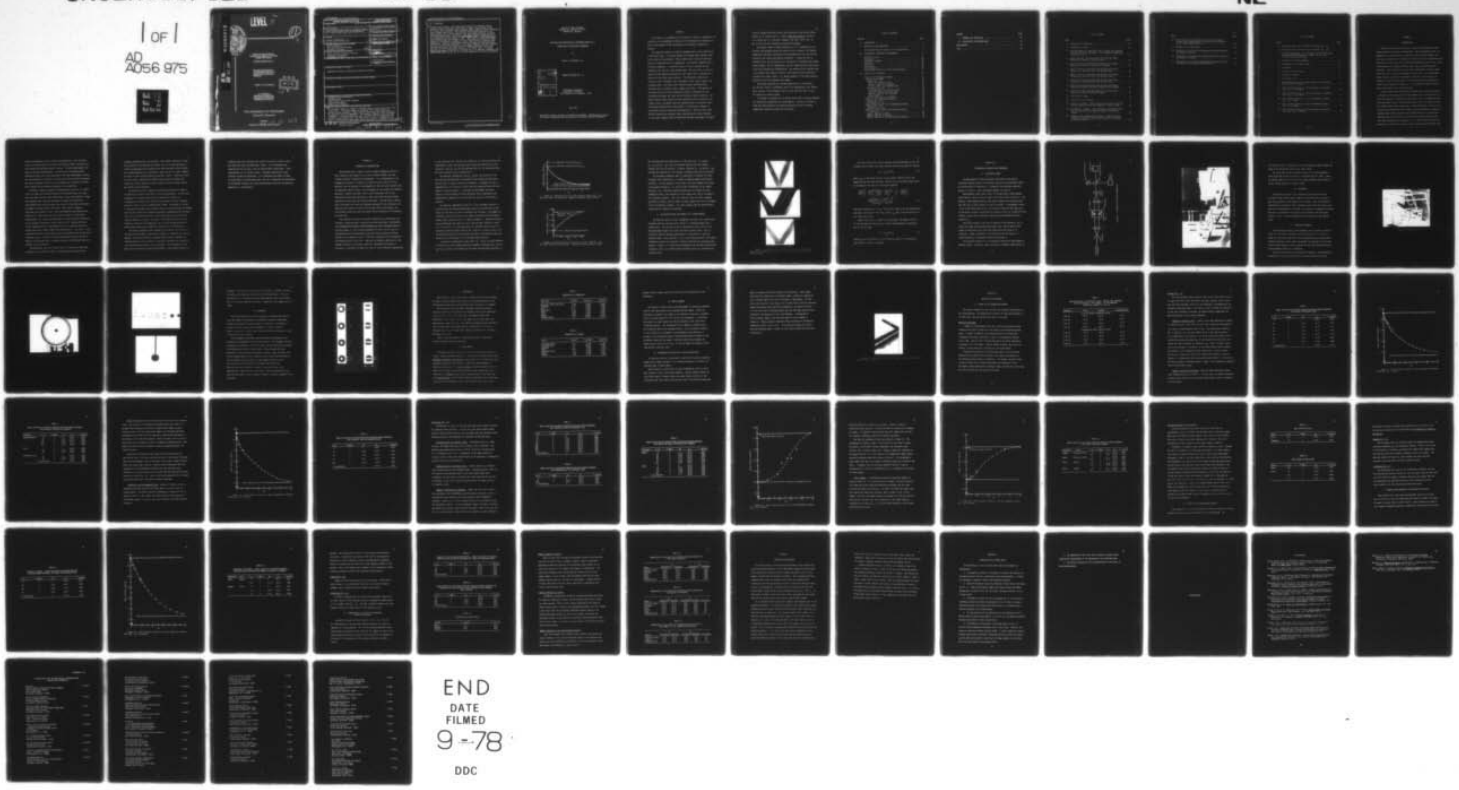

END
DATE FILMED
9-78
DDC

LEVEL II

(11)

OFFICE OF NAVAL RESEARCH
CONTRACT NO. N00014-71-A-0121-0001
PROJECT NO. 384-306

TECHNICAL REPORT NO. 16

RAYLEIGH-LIKE REFLECTION OF ULTRASONIC WAVES AT A LIQUID-SOLID LAYER-SOLID INTERFACE

DANIEL A. McCATHERN, JR.

M.A. BREAZEALE
PRINCIPAL INVESTIGATOR
ULTRASONICS LABORATORY
DEPARTMENT OF PHYSICS

THE UNIVERSITY OF TENNESSEE
Knoxville, Tennessee

JUNE 1978

Unclassified

SECURITY CLASSIFICATION OF THIS PAGE (When Data Entered)

REPORT DOCUMENTATION PAGE

READ INSTRUCTIONS BEFORE COMPLETING FORM

1. REPORT NUMBER: 16

2. GOVT ACCESSION NO.

3. RECIPIENT'S CATALOG NUMBER

4. TITLE (and Subtitle): (6) RAYLEIGH-LIKE REFLECTION OF ULTRASONIC WAVES AT A LIQUID-SOLID LAYER-SOLID INTERFACE

5. TYPE OF REPORT & PERIOD COVERED: (9) Interim technical rept.

6. PERFORMING ORG. REPORT NUMBER

7. AUTHOR(s): (10) Daniel A. McCathern, Jr.

8. CONTRACT OR GRANT NUMBER(s): (15) N00014-76-C-0177, N00014-71-A-0121-0001

9. PERFORMING ORGANIZATION NAME AND ADDRESS
Dept. of Physics
The University of Tennessee
Knoxville, TN 37916

10. PROGRAM ELEMENT, PROJECT, TASK AREA & WORK UNIT NUMBERS: (14) TR-16

11. CONTROLLING OFFICE NAME AND ADDRESS
Office of Naval Research, Code 421
Department of the Navy
Arlington, VA 22217

12. REPORT DATE: (11) June 1978

13. NUMBER OF PAGES: 69 (12) 68 p.

14. MONITORING AGENCY NAME & ADDRESS (if different from Controlling Office)

15. SECURITY CLASS. (of this report): Unclassified

15a. DECLASSIFICATION/DOWNGRADING SCHEDULE

16. DISTRIBUTION STATEMENT (of this Report)

Approved for public release; distribution unlimited.

17. DISTRIBUTION STATEMENT (of the abstract entered in Block 20, if different from Report)

18. SUPPLEMENTARY NOTES

19. KEY WORDS (Continue on reverse side if necessary and identify by block number)
Ultrasonic wave reflection
Rayleigh angle
Liquid-solid layer-solid interface
Leaky surface waves
Surface wave phenomena

20. ABSTRACT (Continue on reverse side if necessary and identify by block number)

An ultrasonic beam in a liquid is incident upon a solid coated with a thin solid layer. At certain angles of incidence leaky surface waves are excited on the interface. These surface waves cause the reflected beam to be separated into two components: the specular component and a displaced component. A schlieren system is used to observe the two components and the null strip between them. The null strip is used as a measure of the angle of excitation of the surface waves, and hence as a measure of the → next page

DD FORM 1 JAN 73 1473 EDITION OF 1 NOV 65 IS OBSOLETE
S/N 0102-LF-014-6601

Unclassified

SECURITY CLASSIFICATION OF THIS PAGE (When Data Entered)

20. Continued

surface wave velocity. The substrates studied were stainless steel, aluminum, lead, plexiglass, brass, glass, copper, and aluminum oxide. The layers were zirconium oxide, aluminum oxide, aluminum, brass, stainless steel, copper, and nickel. The behavior of the phase velocity of the Rayleigh-like waves is determined by the relationship between the layer and the substrate shear velocities. The phase velocity tends toward the layer Rayleigh velocity except for the ceramic layers, zirconium oxide and aluminum oxide, on stainless steel. The behavior observed for these samples is attributed to changes in layer shear velocity resulting from granularity. When the layer shear velocity exceeds the substrate shear velocity and the layer thickness is very small compared with the substrate Rayleigh wavelength, the phase velocity changes much more slowly than indicated by the Farnell-Adler theory [G. W. Farnell and E. L. Adler, Physical Acoustics, edited by W. P. Mason and R. N. Thurston (Academic, New York, 1972), Vol. IX, pp. 35-127] for the vacuum-solid layer-solid problem.

OFFICE OF NAVAL RESEARCH
CONTRACT NO. N00014-76-C-0177
PROJECT NO. 384-306

RAYLEIGH-LIKE REFLECTION OF ULTRASONIC WAVES AT A LIQUID-SOLID LAYER-SOLID INTERFACE

by

Daniel A. McCathern, Jr.

TECHNICAL REPORT NO. 16

Ultrasonics Laboratory
Department of Physics
The University of Tennessee 37916

June 1978

PREFACE

This report is an adaptation of the thesis of Daniel A. McCathern, Jr., submitted to the Department of Physics at The University of Tennessee in partial fulfillment of the requirements of the degree of Master of Science.

An ultrasonic beam in a liquid is incident upon a solid coated with a thin solid layer. At certain angles of incidence leaky surface waves are excited on the interface. These surface waves cause the reflected beam to be separated into two components: the specular component and a displaced component. A schlieren system is used to observe the two components and the null strip between them. The null strip is used as a measure of the angle of excitation of the surface waves, and hence as a measure of the surface wave velocity. The substrates studied were stainless steel, aluminum, lead, plexiglass, brass, glass, copper, and aluminum oxide. The layers were zirconium oxide, aluminum oxide, aluminum, brass, stainless steel, copper, and nickel. The behavior of the phase velocity of the Rayleigh-like waves is determined by the relationship between the layer and the substrate shear velocities. The phase velocity tends toward the layer Rayleigh velocity except for the ceramic layers, zirconium oxide and aluminum oxide, on stainless steel. The behavior observed for these samples is attributed to changes in layer shear velocity resulting from granularity. When the layer shear velocity exceeds the substrate shear velocity and the layer thickness is very small compared with the substrate Rayleigh wavelength, the phase

velocity changes much more slowly than indicated by the Farnell-Adler theory [G. W. Farnell and E. L. Adler, Physical Acoustics, edited by W. P. Mason and R. N. Thurston (Academic, New York, 1972), Vol. IX, pp. 35-127] for the vacuum-solid layer-solid problem.

The author wishes to thank sincerely Dr. M. A. Breazeale for his patience and guidance during the course of this research. His helpful suggestions and advice during both the performance of the work and the writing of the thesis have proven invaluable. A thank you also is extended to Dr. Laszlo Adler for his assistance in obtaining the ceramic-coated samples, for his suggestions, and for submitting the liquid-solid layer-solid problem for consideration. The Nondestructive Testing Group in the Metals and Ceramics Division of Oak Ridge National Laboratory provided the ceramic layers. Dr. Werner Neubauer of the Naval Research Laboratory lent the aluminum oxide sample.

The author expresses his sincere appreciation to his parents, Mr. and Mrs. Daniel A. McCathern, and to his grandparents, Mrs. Thelma Wells and Mrs. Ollie McCathern, for all that they have done to help him during his college career.

The author is grateful to the United States Office of Naval Research for financially supporting this investigation. Finally, he wishes to thank Mrs. Maxine Martin for typing the manuscript and for making suggestions during the course of the writing.

TABLE OF CONTENTS

LIST OF TABLES

TABLE PAGE

LIST OF FIGURES

CHAPTER I

INTRODUCTION

Ultrasonic wave reflection from a liquid-solid interface has been studied extensively by many investigators. Only longitudinal waves can propagate in a liquid because of the low viscosity of the medium, but such waves incident from a liquid onto a solid can excite longitudinal and shear waves in the solid, and a reflected longitudinal wave in the liquid. At some angles of incidence, surface waves can be excited along the interface. Total reflection occurs at the longitudinal critical angle, above which only shear waves propagate in the solid. For solids whose shear velocity exceeds the longitudinal velocity in the liquid, one observes a shear critical angle, at and above which total reflection occurs for all angles of incidence. It is beyond this shear critical angle that surface waves can be excited.

Garber (1966) used a goniometer to measure the reflected energy as a function of incident angle for longitudinal waves incident from water onto flat samples of aluminum and beryllium in order to compare results with calculated values. The experiment agreed well with theory except for certain angles where large dips in reflected energy, attributed to strong energy absorption due to surface wave propagation, were measured. Adequate theoretical explanation for surface waves at a liquid-solid interface was not available at that time, but the existence of such waves was experimentally documented. R. F. Smith (1968) modified the goniometer to allow the receiver to move laterally and discovered that

lateral displacements in the reflected beam parallel to the interface occur for certain angles of incidence for beams incident from water onto the aluminum and duralumin samples studied. Schlieren photographs were taken to show the displacements. The decreases in measured energy observed by Garber were then explained by the beam displacements causing the reflected beam to partially or totally miss the receiving transducer. The results obtained by Smith do not disregard the existence of surface waves because the displacement mechanism is not specified.

Ultrasonic beams of Gaussian distribution were used by J. H. Smith (1971) to study the reflected beam near the Rayleigh angle, the angle above the shear critical angle where energy losses were observed. Using the goniometer and schlieren technique, he found the energy to be redistributed into multiple beams, one or more of which may be dominant. The samples studied in water were brass, lead, lucite, aluminum, beryllium, and stainless steel. Some investigators had attributed the energy losses noted above the shear critical angle to lateral beam displacements, but energy redistribution is a more accurate description of the situation (Breazeale, Adler, Smith, 1975). Bertoni and Tamir (1973) suggested that this phenomenon was due to coupling between the incident wave and a leaky surface wave excited by it. The energy is then reradiated from this leaky surface wave and interferes with the specularly reflected energy. The angle at which the surface waves are excited is known as the Rayleigh angle, although originally the Rayleigh angle was defined for free surfaces.

The goniometer was used by Scott (1975) to measure the amplitude and phase near the Rayleigh angle of Gaussian beams reflected from

aluminum, aluminum oxide, and stainless steel samples immersed in water. He explained that attributing the energy loss at the Rayleigh angle to lateral displacement after examining the water-aluminum interface might be an understandably easy conclusion to draw, but for the other samples, only part of the reflected beam was observed to shift. Breazeale, Adler, and Scott (1977) supported the Bertoni-Tamir theory by showing that indeed the incident beam does couple resonantly with the leaky surface wave before being reradiated.

An extension of the liquid-solid interface problem can be made by the addition of a thin solid layer to the solid substrate. Elastic wave propagation in layered media has been a problem of interest to seismologists for many years, and has been treated by Ewing, Jardetsky, and Press (1957) as well as Brekhovskikh (1960). At present, no theory is available for predicting the phase velocity of the Rayleigh-like surface wave for the liquid-solid layer-solid problem, although Farnell and Adler (1972) have treated the case for a thin solid layer on a substrate of infinite depth in a vacuum. Not only is the liquid-solid layer-solid problem of interest to seismologists, but it also has applications to surface wave devices and to materials testing for coated materials.

The primary purpose of this research is to observe the behavior of the phase velocity when a thin layer is added to a substrate in a liquid medium. The optical schlieren technique can be used to identify the Rayleigh angles to the interfaces of interest from which the velocities of the Rayleigh-like modes can be calculated. Then comparison can be made to the vacuum-solid layer-solid problem. A preliminary report for

aluminum oxide and zirconium oxide layers on stainless steel in water has been made (Adler and McCathern, 1978). It was announced that observations did not agree with the Farnell-Adler predictions. These observations will be further tested. Secondary objectives of this research include the following: (1) to determine the effect of beam size and shape on the Rayleigh angle, and (2) to determine the reliability of the Überall equation for predicting Rayleigh velocities for materials immersed in a liquid medium.

CHAPTER II

THEORETICAL CONSIDERATIONS

The Rayleigh wave, a mode of elastic energy propagation which can exist along the free surface of a solid of infinite depth, has been studied in detail by numerous investigators. It is nondispersive, the propagation velocity is slightly less than the shear velocity of the material, and the mechanical displacements of the wave decay exponentially to negligible values within a few wavelengths of the surface for isotropic materials. Farnell and Adler (1972) treat the general case of the Rayleigh-like mode upon addition of a thin solid layer having intimate mechanical contact with the infinite substrate. The thin layers usually have a thickness less than the Rayleigh wavelength of the substrate, and when they are placed in contact with the previously free surface, the wave becomes dispersive since the phase velocity depends on the frequency of excitation.

The equations of motion are greatly simplified by considering only isotropic, nonpiezoelectric substrate and layer materials. The solutions to be obtained are straight-crested propagating waves with phase velocity V and wave number K. The traction components of stress and the particle displacements must be continuous across the layer-substrate interface because of the intimate contact. Electrical conditions can be neglected for nonpiezoelectric materials. Applying the boundary conditions to the assumed solutions, two extreme limits are encountered which make it necessary to distinguish between two types of layer-substrate combinations.

In the discussion that follows, the symbols V_L, V_S, and V_R represent the longitudinal, shear, and Rayleigh wave velocities respectively of the substrate, while $\hat{V}_L$, $\hat{V}_S$, and $\hat{V}_R$ represent those of the layered material. The layer thickness will be denoted by h.

For material combinations with $\hat{V}_S < V_S/\sqrt{2}$, the velocity of the free-surface Rayleigh mode is decreased by the presence of the layer, and the layer is said to "load" the substrate. An example of such a combination is zinc oxide on silicon, and the dispersion curve for this sample is given in Figure 1. According to this graph, the phase velocity of the Rayleigh-like mode decreases with increasing Kh and asymptotically approaches the layer Rayleigh velocity as Kh tends to infinity.

For material combinations with $\hat{V}_S > \sqrt{2}\ V_S$, the phase velocity is increased over the substrate Rayleigh velocity by the presence of the layer, and the layer is said to "stiffen" the substrate. An example of stiffening would be silicon on zinc oxide, the reverse of the previous sample, whose dispersion curve is shown in Figure 2. Characteristically, only one Rayleigh-like mode can exist, and the phase velocity V starts at $V = V_R$ for $Kh = 0$, increasing until the substrate shear velocity is reached at some particular value of Kh. Thus for a limited range of Kh, the minimum velocity of the Rayleigh-like mode is the substrate Rayleigh velocity, and the maximum is the substrate shear velocity.

For material combinations with $V_S/\sqrt{2} < \hat{V}_S < \sqrt{2}\ V_S$, the same behavior is noted as for the strongly loading or strongly stiffening case, even if $\hat{V}_S \simeq V_S$, as long as the ordering of the shear and Rayleigh velocities of

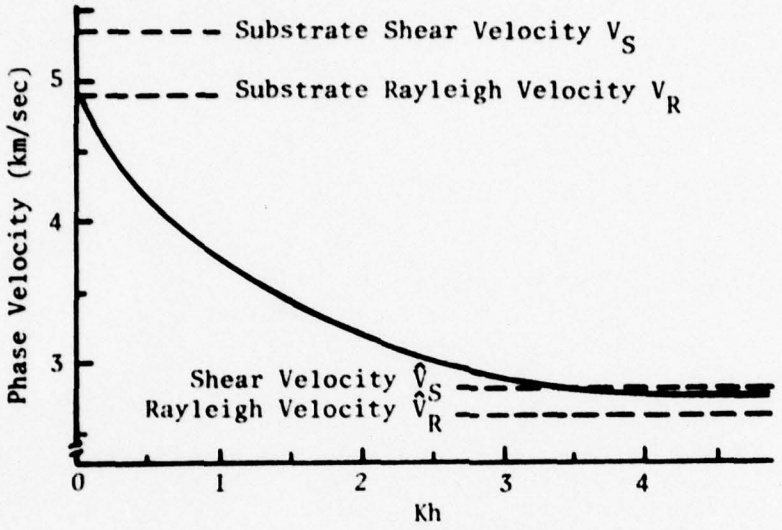

Figure 1. Dispersion curve for zinc oxide on silicon ($\hat{V}_S < V_S$). The layer loads the substrate. (Farnell and Adler, 1972, p. 56.)

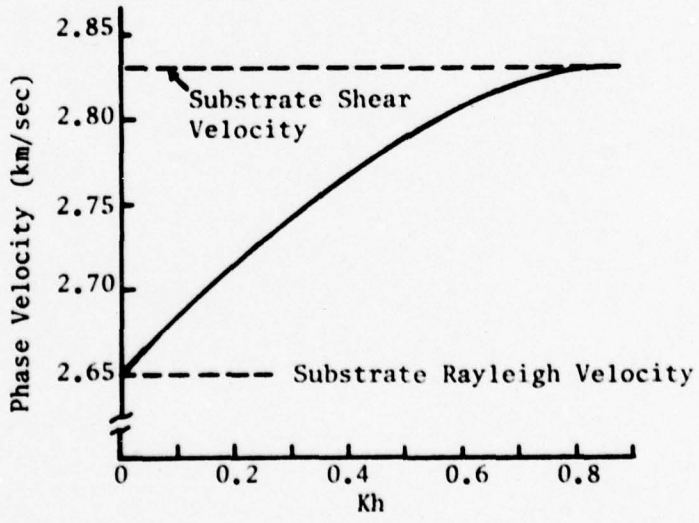

Figure 2. Dispersion curve for silicon on zinc oxide ($\hat{V}_S > V_S$). The layer stiffens the substrate. (Farnell and Adler, 1972, p. 53.)

the substrate and layer materials is as for that case. As long as $\hat{V}_S < V_S$ (and $\hat{V}_R < V_R$), then the behavior expected for the strongly loading case will be observed. Likewise, whenever $\hat{V}_S > V_S$ (and $\hat{V}_R > V_R$), the behavior expected for the strongly stiffening case will be observed.

The preceding statements make it convenient to redefine the terms "loading" and "stiffening" in a slightly different manner from Farnell and Adler. For the purposes of this work, the term "loading" will apply to any sample having $\hat{V}_S < V_S$, and the term "stiffening" to any sample having $\hat{V}_S > V_S$. With this expanded definition, the copper on steel, aluminum on glass, and aluminum on steel samples will now be included in the "loading" category. Also, the zirconium oxide on steel, aluminum and steel on copper, and the copper on brass samples will all be included in the "stiffening" category. All other samples obey the Farnell-Adler conditions for loading or stiffening.

A. THE RAYLEIGH MODE FOR SAMPLES IN A LIQUID MEDIUM

The Rayleigh mode of energy propagation can exist at a liquid-solid interface when the incident wave couples in a resonant manner with a surface wave. The excitation of the Rayleigh wave takes place at the Rayleigh angle located just above the shear critical angle. When an ultrasonic beam of Gaussian distribution is incident at or near the Rayleigh angle to the interface, a null strip resulting from a 180° phase difference between the specularly reflected beam and the reradiated wave appears. Figure 3 is a schlieren photograph of the incident and reflected ultrasonic beams at a water-aluminum interface below, at, and above the Rayleigh angle.

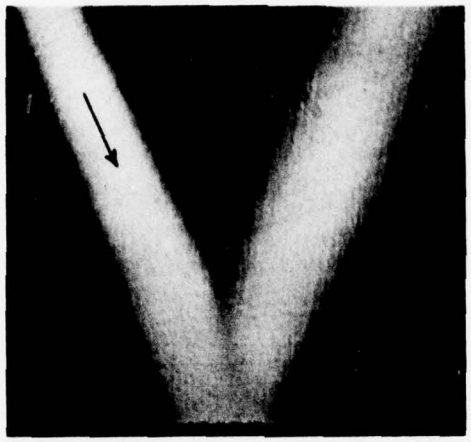

(a)
$\theta = 20°$

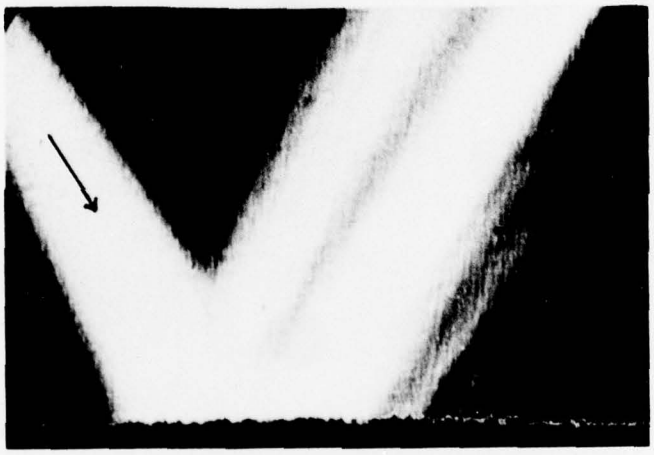

(b)
$\theta_R = 31°$

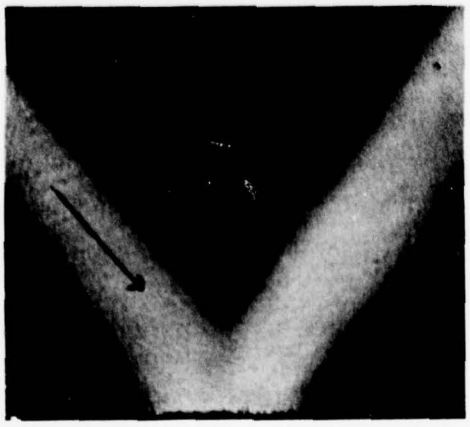

(c)
$\theta = 35°$

Figure 3. Schlieren photograph of an ultrasonic beam incident upon a water-aluminum interface (a) below, (b) at, and (c) above the Rayleigh angle.

The null strip can be used to measure the Rayleigh angle θ_R for the interface and to obtain the leaky Rayleigh velocity V_R using the equation

$$V_R = V_{liq}/\sin \theta_R \tag{1}$$

where V_{liq} is the sound velocity in the liquid. Überall (1973) has suggested that the leaky Rayleigh velocity can be calculated from theory by solving for the roots of the secular equation

$$4\left(\frac{V_S}{C}\right)^2\left[1 - \left(\frac{V_S}{C}\right)^2\right]^{1/2}\left[\left(\frac{V_S}{V_L}\right)^2 - \left(\frac{V_S}{C}\right)^2\right]^{1/2} + \left[1 - 2\left(\frac{V_S}{C}\right)^2\right]^2 = - \frac{\rho_{liq}}{\rho}\left[\frac{(V_S/V_L)^2 - (V_S/C)^2}{(V_S/V_{liq})^2 - (V_S/C)^2}\right]^{1/2} \tag{2}$$

where one solution for C is V_R. The terms V_L and V_S are the longitudinal and shear velocities of the solid, while ρ_{liq} and ρ are the densities of the liquid and solid.

When a thin layer is added to the substrate, the phase velocity V of the Rayleigh-like mode can be obtained experimentally by modifying Eq. (1) to the form

$$V = V_{liq}/\sin \theta_R \tag{3}$$

where θ_R, still referred to as the "Rayleigh angle," is the angle at which the null strip is observed.

CHAPTER III

EXPERIMENTAL APPARATUS AND PROCEDURE

A. SCHLIEREN SYSTEM

All measurements of Rayleigh angles were made by the optical schlieren technique using the schlieren system of the Ultrasonics Group at The University of Tennessee. A diagram of the schlieren apparatus appears in Figure 4, and a photograph appears in Figure 5.

Monochromatic light from a laser is incident upon a beam expander which creates a point source of light at the focal point of lens L_1. The parallel light emerging from L_1 then passes through the schlieren tank and into lens L_2 which focuses it back to a point. A transparent screen is set in the focal plane of L_2, and a spot of India ink the same size as the point of light is placed on the screen to serve as a spatial filter. Finally, a prism and a television camera are placed behind the focal plane of L_2.

Any object placed in the beam of parallel light between L_1 and L_2 causes the light to bend around the opaque spot, and an image of the object is received by the television camera when the prism is in position 1. When in position 2, the prism diverts the image into a camera mounted on a tripod for taking still pictures.

An ultrasonic beam acts as a diffraction grating for monochromatic, parallel light. Therefore, light striking an ultrasonic beam present in

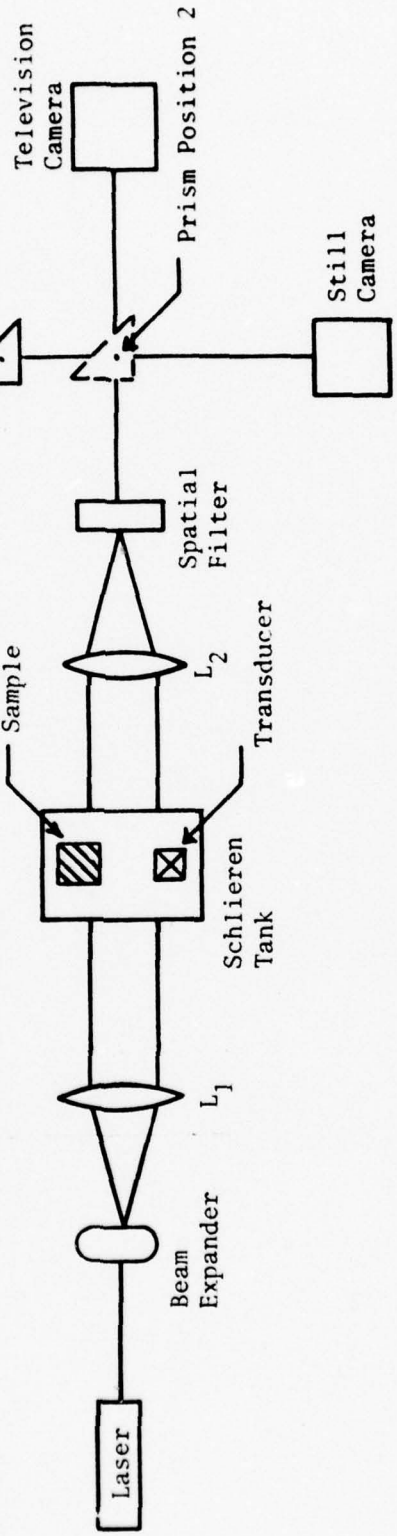

Figure 4. Diagram of schlieren apparatus.

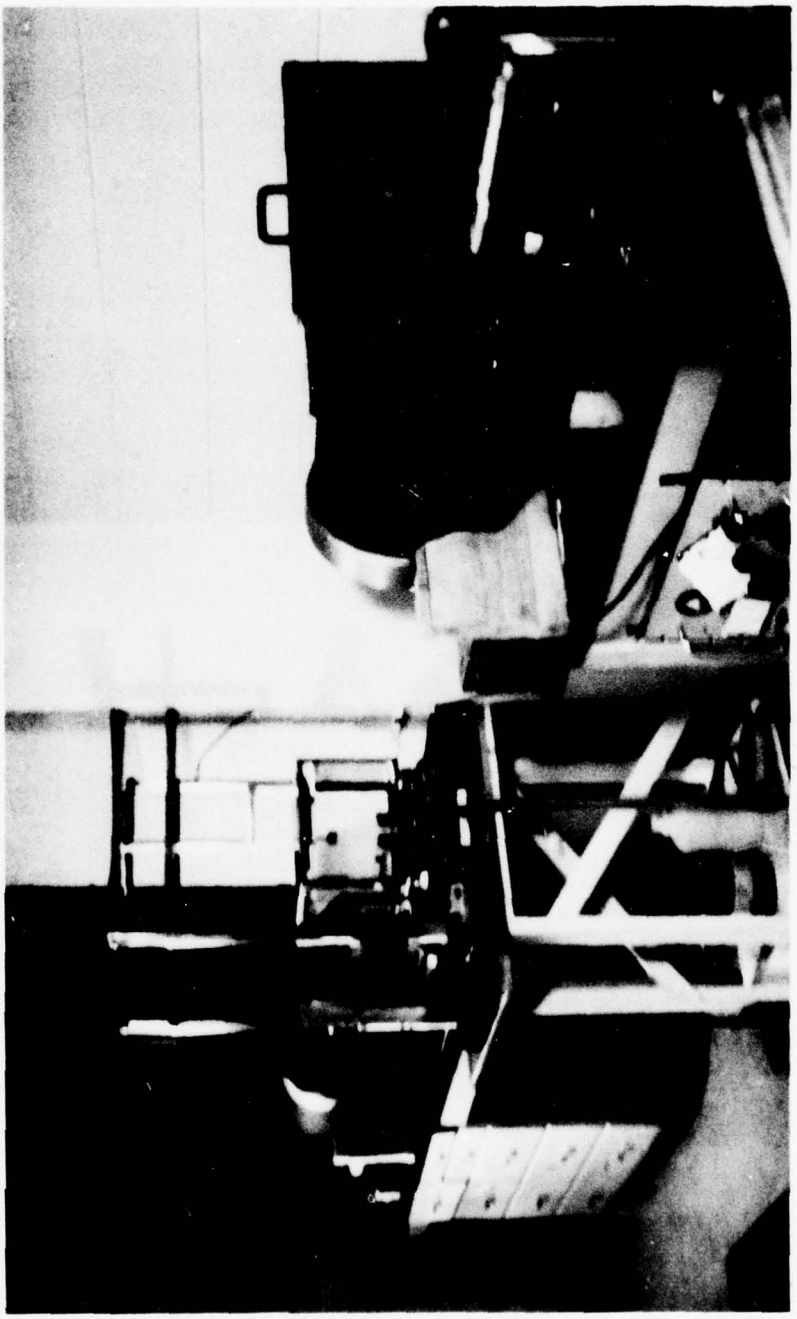

Figure 5. Photograph of schlieren system.

the schlieren tank is diffracted, and the diffraction orders produce an image of the ultrasonic beam on the video screen.

The laser used in the schlieren system is a 0.5 mw Helium-Neon laser producing visible red light of wavelength 6328 Å. Both L_1 and L_2 are Eastman Kodak f/6.3 48-inch focal length Telephoto Type I-Class B lenses, having apertures of eight inches.

B. GONIOMETER

An important feature of the schlieren system used is that an ultrasonic beam incident upon a sample in the tank will be incident upon the same point of the sample at all angles. This is achieved by suspending the transducer from a goniometer built over the tank in the form of a parallelopiped. The angle of incidence is changed by the worm gear and is measured by the angular scale located on the worm gear. Figures 6 and 7 show the goniometer and a close-up of the angular scale.

C. TRANSDUCER ASSEMBLY

The transducer assembly used throughout this research is shown in Figure 8. The brass transducer consists basically of a cylindrical front cap fitted onto the rear case and sealed with an O-ring fixture, thereby providing a water-tight compartment for housing the electrodes and for protecting the contact between the cable and electrode from the liquid medium in which it is immersed.

The device facilitates the changing of frequency, accomplished by removing the front cap and inserting a crystal having the desired

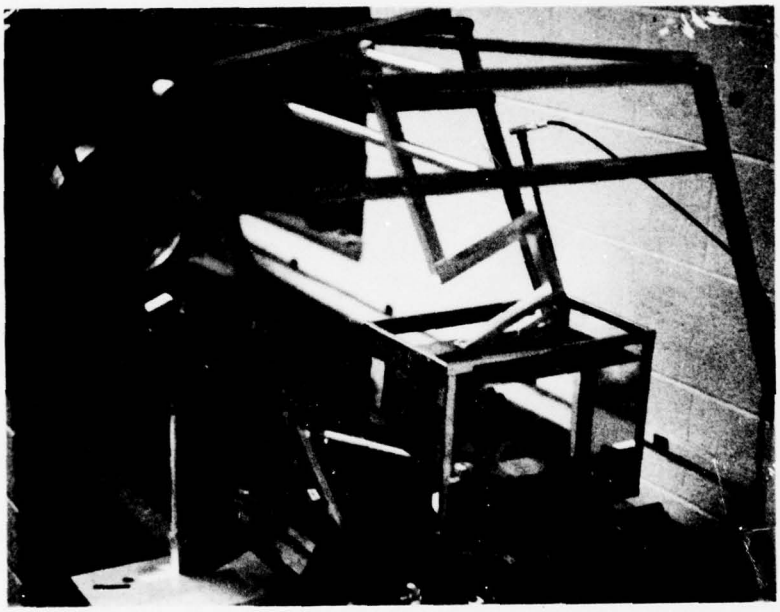

Figure 6. Goniometer.

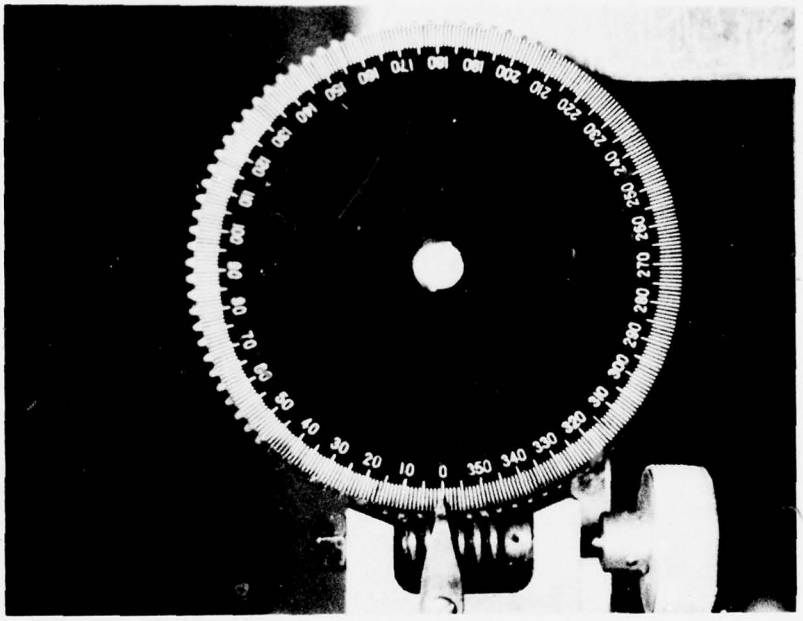

Figure 7. Close-up of angular scale.

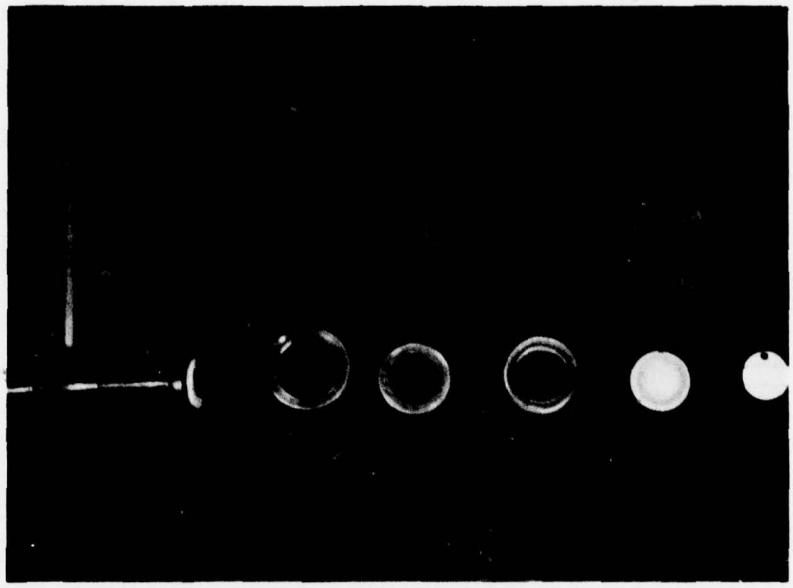

(a)

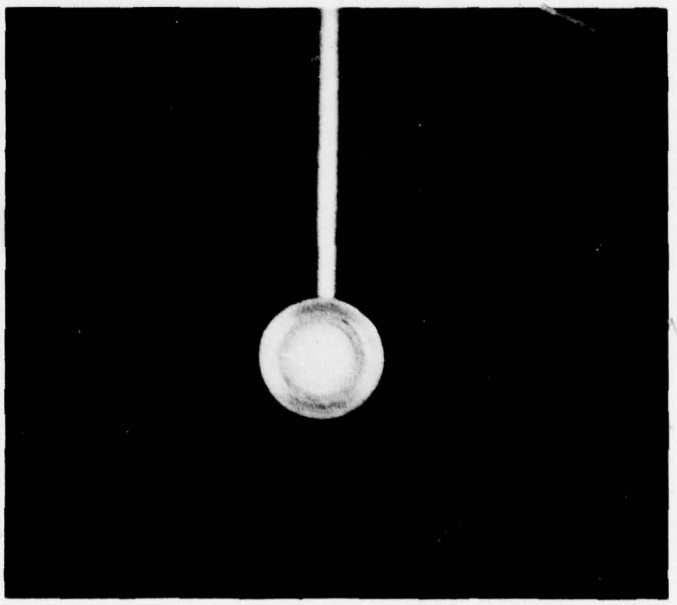

(b)

Figure 8. Transducer assembly.

frequency. The crystals used were all X-cut quartz crystals, one-inch in diameter and coated on one side with a thin gold layer. The conducting layer is in contact with the liquid medium, while the uncoated side is in contact with the electrode. Frequencies used ranged from 1 to 7 MHz.

D. ELECTRODES

One of the objectives of this study was to determine how various sizes and shapes of electrodes, and therefore incident sound beams, influence the measured Rayleigh angle of a material. Accordingly, a variety of brass circular and rectangular electrodes, shown in Figure 9, was used. Teflon rings served to hold the electrodes in place in the center of the crystal.

The rectangular electrodes used by previous investigators were replaced by well-machined ones for this project. The alignment of these rectangular electrodes is a critical point, for the ultrasonic beam must be perpendicular to the incoming light. Grooves having the same dimensions as the electrodes were made in teflon rings, and holes were drilled through them for the cylindrical projections from the backs of the electrodes to pass in order to make contact with the cable. The transducer was fitted with an alignment pin projecting from the rear case (visible in Figure 8), and each teflon ring supplied with a hole near the outer edge so that matching the pin and hole during assembly of the transducer results in proper alignment of the electrode.

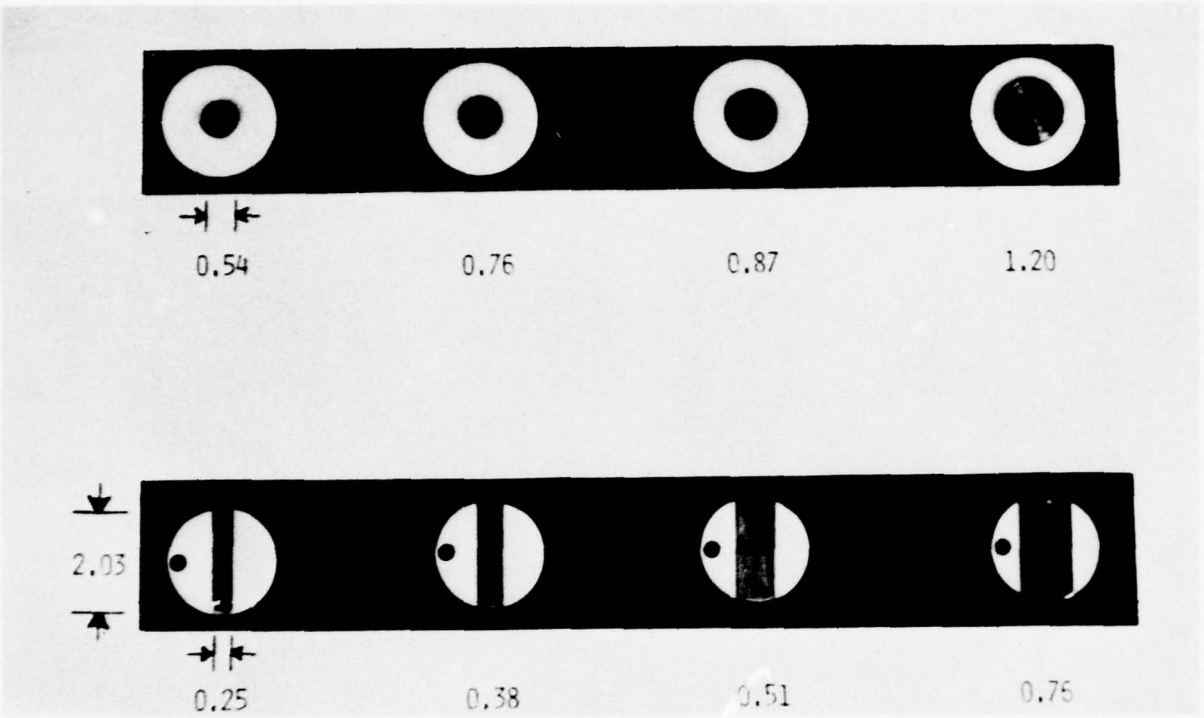

Figure 9. Electrodes (cm).

E. SUBSTRATES

Many substrates with a wide range of shear velocities were chosen in order to better examine the behavior of the Rayleigh angle as the differential between layer and substrate shear velocities is changed.

The stainless steel type 304L, aluminum, lead and plexiglass substrates were all in the form of rectangular blocks with dimensions 10 cm x 5 cm x 2.5 cm. The brass was a rectangular block with dimensions 7 cm x 5 cm x 2.5 cm. The glass was in cubic form, each edge having a length of 5 cm. The copper and aluminum oxide substrates were circular disks, the former having a diameter of 7.5 cm and a thickness of 1.3 cm, and the latter having a diameter of 6.5 cm and a thickness of 2.6 cm.

Table 1 lists the density, longitudinal velocity, and shear velocity measured for each substrate.

F. THIN LAYERS

The materials used as thin layers in this research are listed in Table 2 along with their properties. Values were obtained from the CRC Handbook of Chemistry and Physics, except those for zirconium oxide and aluminum oxide which were measured. Basically, three methods of deposition were used: (1) spray coating, in which the material to be deposited is heated to the melting point and then sprayed onto the substrate, (2) bonding using silicone vacuum grease as the bond, and (3) electroplating. The zirconium oxide and aluminum oxide layers were spray coated, the aluminum, brass, and stainless steel layers were

TABLE 1

PROPERTIES OF SUBSTRATES

Substrate	ρ (g/cm^3)	V_L (m/sec)	V_S (m/sec)
Stainless Steel Type 304L	8.09	5,610	3,180
Aluminum	2.73	6,400	3,100
Lead	11.4	1,960	690
Plexiglass	1.24	2,590	1,290
Brass	8.86	4,150	2,050
Glass	2.66	5,660	3,370
Copper	8.93	5,010	2,270
Aluminum Oxide	4.0	10,460	6,010

TABLE 2

PROPERTIES OF LAYERS

Layer	ρ (g/cm^3)	V_L (m/sec)	V_S (m/sec)
Zirconium Oxide	5.2	7,660	4,300
Aluminum Oxide	4.0	10,460	6,010
Aluminum	2.7	6,420	3,040
Brass	8.6	4,700	2,110
Stainless Steel	7.9	5,790	3,100
Copper	8.93	5,010	2,270
Nickel	8.85	5,480	2,990

bonded, and the copper and nickel layers were electroplated onto the substrates.

G. BEAM ALIGNMENT

The system is zeroed before each measurement by setting up standing waves in the tank between the transducer and the sample. After the transducer is mounted, the sample to be studied is placed on a platform with its surface parallel to the face of the transducer. A traveling microscope is placed behind the tank and focused on the sound field visibility pattern. The orientation of the sample is adjusted until the visibility pattern has optimum clarity. As the visibility pattern is very sensitive to alignment of the transducer and reflector, it becomes a very convenient means of establishing normal incidence of the ultrasonic beam onto the sample. With the system thus aligned, the angular scale can be set to zero, so that the angle of incidence can be read directly from the scale.

H. EXPERIMENTAL DEFINITION OF THE RAYLEIGH ANGLE

In practice, the null strip used to identify the Rayleigh angle may appear over a range of angles, so it becomes necessary to pinpoint the Rayleigh angle by other means.

Most materials, particularly at lower frequencies such as 2 and 3 MHz, exhibit a rather interesting behavior. Several degrees before the null strip begins to appear, many very narrow beams, parallel to the reflected beam, split apart from the main body of the reflected beam and

begin to spread out over the surface of the material. These beams, which shall be referred to as secondary beams, increase in number and cover a larger area as the null strip range is approached. At some point within the null strip range, the secondary beams reach their maximum number and spread, after which they diminish as the angle increases. It is at this point of maximum spread that the Rayleigh angle has been defined for the purposes of this investigation. A photograph of these secondary beams at the Rayleigh angle of steel appears in Figure 10. These secondary beams have been attributed to diffraction (Breazeale, Adler, Scott, 1977). If no secondary beams are visible, then the Rayleigh angle is chosen as that angle at which the best null strip occurs.

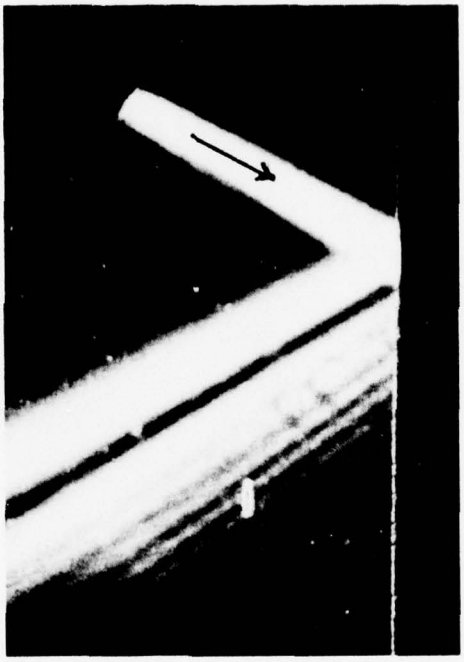

Figure 10. Photograph showing the secondary beams at the Rayleigh angle of steel in water.

CHAPTER IV

RESULTS AND DISCUSSION

A. WATER AS THE PROPAGATING MEDIUM

The results reported in this section were obtained using water as the liquid medium. The longitudinal velocity of water was measured to be 1482 m/sec, and the density was taken as 1.0 g/cm^3.

Beam Size and Shape

A number of investigators have used circular electrodes without examining the effect of beam size and shape on the measured Rayleigh angle. A number of samples were examined using the circular and rectangular electrodes described on page 17 at frequencies between 1 and 7 MHz. Table 3 lists the Rayleigh angles for three substrates irradiated with 2 MHz beams. Similar behavior results for other substrates, layered materials, frequencies, and liquid media.

Although the magnitude of the Rayleigh angle is not noticeably affected by the shape of the electrode, the energy distribution in the reflected beam possibly is affected. For example, the null strip is usually wider with circular beams than with rectangular beams, rectangular beams produce more secondary beams, and the null strip range may vary with the size and shape of the beam.

TABLE 3

RAYLEIGH ANGLES FOR STAINLESS STEEL, COPPER, AND ALUMINUM OXIDE FOR SEVERAL 2 MHz BEAMS. ALL RECTANGULAR BEAMS HAVE LENGTHS OF 2.03 cm

Dimension	Steel	Copper	Aluminum Oxide
	Circular Beams (Diameters Given)		
0.54 cm	30.5°	46.3°	15.5°
0.76 cm	30.5°	46.3°	15.5°
0.87 cm	30.7°	46.5°	15.7°
1.20 cm	30.5°	46.3°	15.7°
	Rectangular Beams (Widths Given)		
0.25 cm	30.5°	46.3°	15.5°
0.38 cm	30.5°	46.3°	15.5°
0.51 cm	30.5°	46.3°	15.5°
0.76 cm	30.5°	46.3°	15.5°

Loading ($\hat{V}_S < V_S$)

The Farnell-Adler theory predicts that if the layer shear velocity is lower than that of the substrate, the phase velocity will be lower than the leaky Rayleigh velocity of the substrate, corresponding to an increase in Rayleigh angle. The layer is said to "load" the substrate. As the layer thickness increases, the phase velocity approaches the Rayleigh velocity of the layered material.

Copper on stainless steel. Table 4 lists data obtained for copper on stainless steel. The phase velocity V was calculated from Equation 3 on page 10 using measured values of θ_R. The dimensionless quantity $Kh = 2\pi \frac{h}{\lambda_R}$ where K is the wave number and h is the layer thickness, is an indication of the relative size of the layer with respect to the substrate Rayleigh wavelength λ_R, for the larger the value of Kh, the larger the layer thickness is compared to λ_R. Table 4 clearly shows that as Kh increases, V decreases as the Farnell-Adler theory predicts for loading in the vacuum-solid layer-solid case. A plot of phase velocity as a function of Kh for the copper-steel sample is given in Figure 11. Although the only data available were for $Kh < 1$, the curve has been extended to resemble Figure 1, page 7, thus showing the expected trend as Kh becomes larger.

Samples loaded with aluminum. Data for three substrates loaded with aluminum are given in Table 5. In each case, the observed behavior parallels that predicted by the Farnell-Adler theory, since V decreases as Kh increases.

TABLE 4

PHASE VELOCITIES CALCULATED FROM THE RAYLEIGH ANGLES MEASURED FOR COPPER ON STAINLESS STEEL

h (μ)	f (MHz)	Kh	θ_R	V (m/sec)
0	2	0	30.5°	2920
20	2	0.10	31.7°	2820
50	2	0.22	32.3°	2775
69	2	0.30	32.7°	2745
69	3	0.45	33.0°	2720
69	4	0.59	34.0°	2650
69	5	0.74	34.9°	2590
∞ (calculated)		∞	44.0°	2135

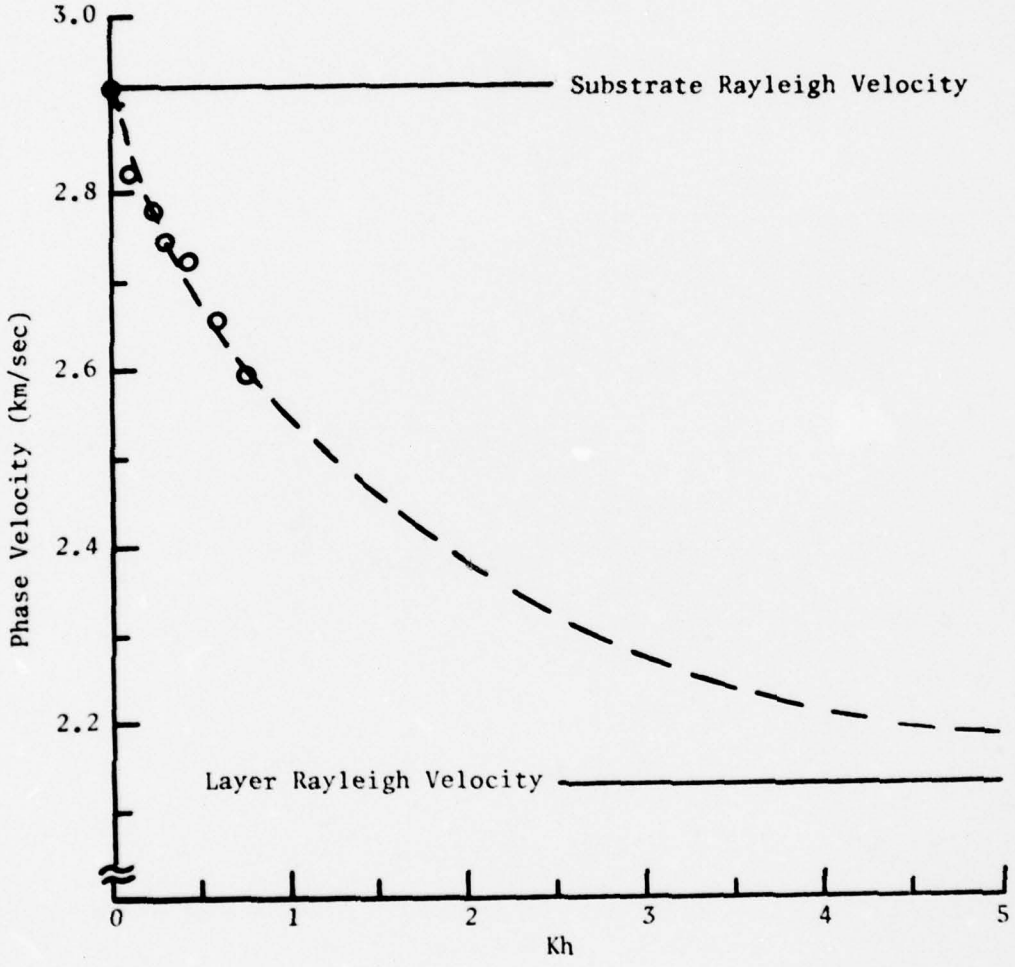

Figure 11. Plot of phase velocity vs. Kh for copper on stainless steel ($V_S < V_S$) in water.

TABLE 5

PHASE VELOCITIES CALCULATED FROM THE RAYLEIGH ANGLES MEASURED FOR MATERIALS LOADED WITH ALUMINUM

Substrate	h (μ)	f (MHz)	Kh	θ_R	V (m/sec)
Aluminum Oxide	0	2	0	15.5°	5545
	20	2	0.05	15.5°	5545
	58	2	0.13	16.3°	5280
	215	2	0.49	17.5°	4930
	215	5	1.22	18.7°	4620
Glass	0	2	0	28.5°	3105
	29	2	0.12	29.0°	3055
	58	2	0.24	30.0°	2965
Stainless Steel	0	2	0	30.5°	2920
	29	2	0.12	31.3°	2855
	29	3	0.19	31.5°	2835
	∞ (calculated)		∞	32.0°	2795

Aluminum oxide has nearly twice the shear velocity of the aluminum layer. The 20μ layer on aluminum oxide demonstrates that there is a minimum layer thickness below which no appreciable change in phase velocity occurs. For this particular sample, the substrate Rayleigh wavelength is 140 times the layer thickness, and the Rayleigh angle is the same as if no layer were present. Refer to Figure 12 for a plot of phase velocity as a function of Kh for aluminum on aluminum oxide. Here again, the curve has been extended to show the expected behavior for larger Kh values.

The other two substrates have shear velocities much closer to that of the layer. The shear velocity of glass is only about 10% higher that that of aluminum, while V_S for steel is very near, though slightly above, the layer shear velocity. Data for these substrates show that regardless of the differential between layer and substrate shear velocities, the phase velocity will be lower than the substrate Rayleigh velocity as long as $\hat{V}_S < V_S$. This is the result expected for the vacuum-solid layer-solid case considered by Farnell and Adler.

Stainless steel on aluminum oxide. Layers of stainless steel on aluminum oxide were examined with 2 MHz beams to further study the loading effect. The phase velocities obtained as a function of Kh are listed in Table 6. Once again, the smallest layer (25μ) produces no measureable change in velocity, and as Kh increases, the phase velocity decreases.

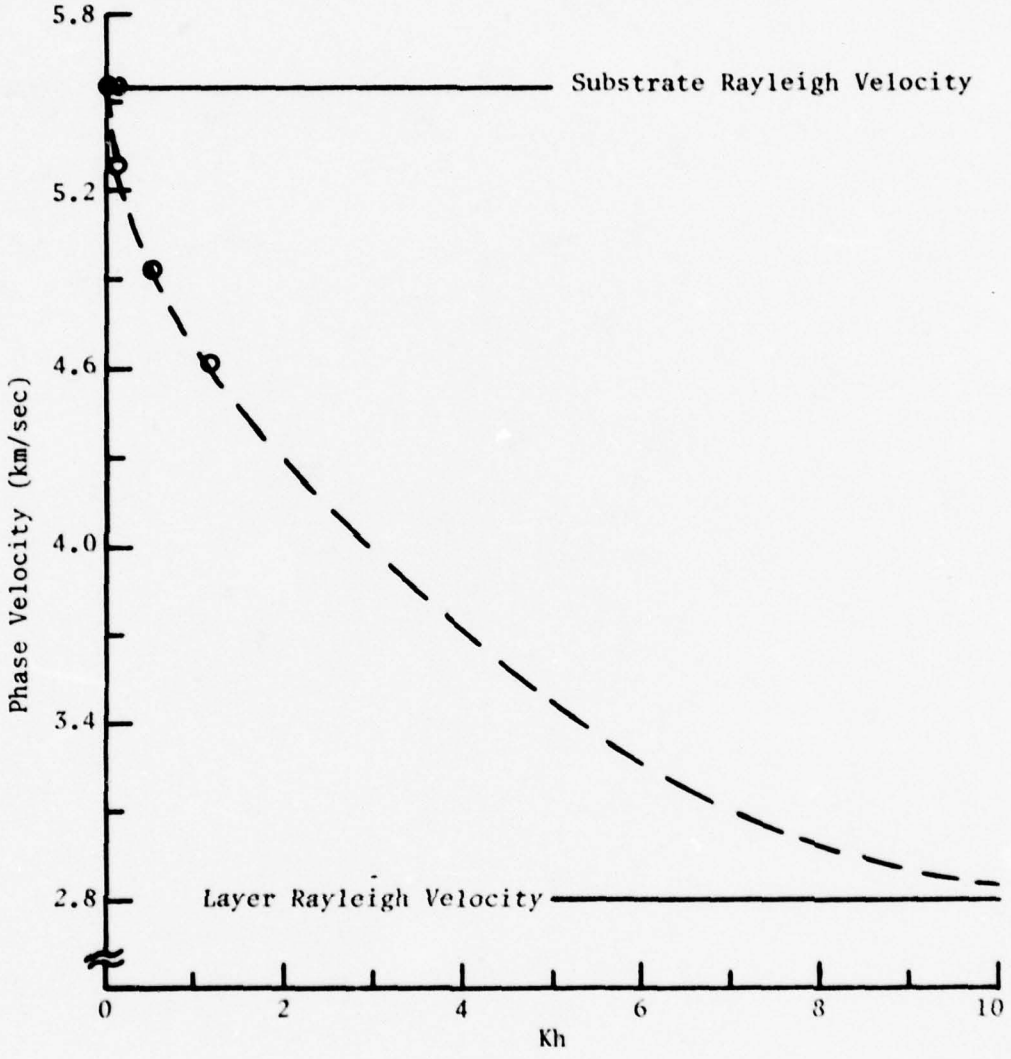

Figure 12. Plot of phase velocity vs. Kh for aluminum on aluminum oxide ($\hat{V}_S < V_S$) in water.

TABLE 6

PHASE VELOCITIES CALCULATED FROM THE RAYLEIGH ANGLES MEASURED FOR STAINLESS STEEL ON ALUMINUM OXIDE

h (μ)	f (MHz)	Kh	θ_R	V (m/sec)
0	2	0	15.5°	5545
25	2	0.06	15.5°	5545
51	2	0.12	16.0°	5375
76	2	0.17	16.3°	5280
102	2	0.23	17.0°	5070
∞ (calculated)		∞	31.0°	2875

Stiffening ($\hat{V}_S > V_S$)

"Stiffening" is said to occur when the layer shear velocity exceeds the substrate shear velocity. In this case, the Farnell-Adler theory predicts that the phase velocity will be higher than the substrate leaky Rayleigh velocity, corresponding to a decrease in Rayleigh angle.

Zirconium oxide on stainless steel. Zirconium oxide has a shear velocity 35% higher than that of the stainless steel substrate. The Rayleigh angle measured for steel is 30.5°, while for zirconium oxide it is calculated to be 21.9°. Examination of the phase velocities listed in Table 7 shows that they decrease as Kh increases, an unexpected result on the basis of the theory.

Aluminum oxide on stainless steel. Earlier (page 31), stainless steel was observed to load aluminum oxide. Choosing stainless steel as the substrate and aluminum oxide as the layer should then cause stiffening, but the results in Table 8 are those expected for the case of loading. Recall that aluminum oxide has twice the shear velocity of stainless steel.

Samples stiffened with aluminum. Copper and brass were layered with aluminum to test stiffening, and the results are given in Table 9. The Rayleigh angle decreases for both materials when stiffened by aluminum. Figure 13 is a plot of phase velocity V as a function of Kh for aluminum on copper. The plot resembles Figure 2 on page 7 in that V approaches the substrate shear velocity for small values of Kh, but near Kh = 0, the data points indicate that the curvature is quite different

TABLE 7

PHASE VELOCITIES CALCULATED FROM THE RAYLEIGH ANGLES MEASURED FOR ZIRCONIUM OXIDE ON STAINLESS STEEL

h (μ)	f (MHz)	Kh	θ_R	V (m/sec)
0	2	0	30.5°	2920
25	2	0.11	31.0°	2880
25	3	0.16	31.0°	2880
75	2	0.32	31.5°	2835
150	2	0.65	32.5°	2760
150	3	0.97	33.0°	2720
250	2	1.08	34.5°	2615
250	3	1.61	34.5°	2615
250	4	2.15	34.5°	2615
∞ (calculated)		∞	21.9°	3975

TABLE 8

PHASE VELOCITIES CALCULATED FROM THE RAYLEIGH ANGLES MEASURED FOR ALUMINUM OXIDE ON STAINLESS STEEL

h (μ)	f (MHz)	Kh	θ_R	V (m/sec)
0	2	0	30.5°	2920
50	2	0.22	31.3°	2850
100	2	0.43	35.0°	2585
∞ (calculated)		∞	15.5°	5545

TABLE 9

PHASE VELOCITIES CALCULATED FROM THE RAYLEIGH ANGLES MEASURED FOR COPPER AND BRASS STIFFENED WITH ALUMINUM

Substrate	h (μ)	f (MHz)	Kh	θ_R	V (m/sec)
Copper	0	2	0	46.3°	2050
	29	2	0.18	46.0°	2060
	58	2	0.36	45.3°	2085
	29	5	0.44	44.0°	2135
	87	2	0.54	43.5°	2155
	29	7	0.62	43.5°	2155
	116	2	0.72	42.5°	2195
Brass	0	2	0	50.0°	1935
	20	2	0.13	50.0°	1935
	29	2	0.19	49.7°	1945
	58	2	0.38	48.9°	1965
	215	2	1.40	46.5°	2045
	∞ (calculated)		∞	32.0°	2795

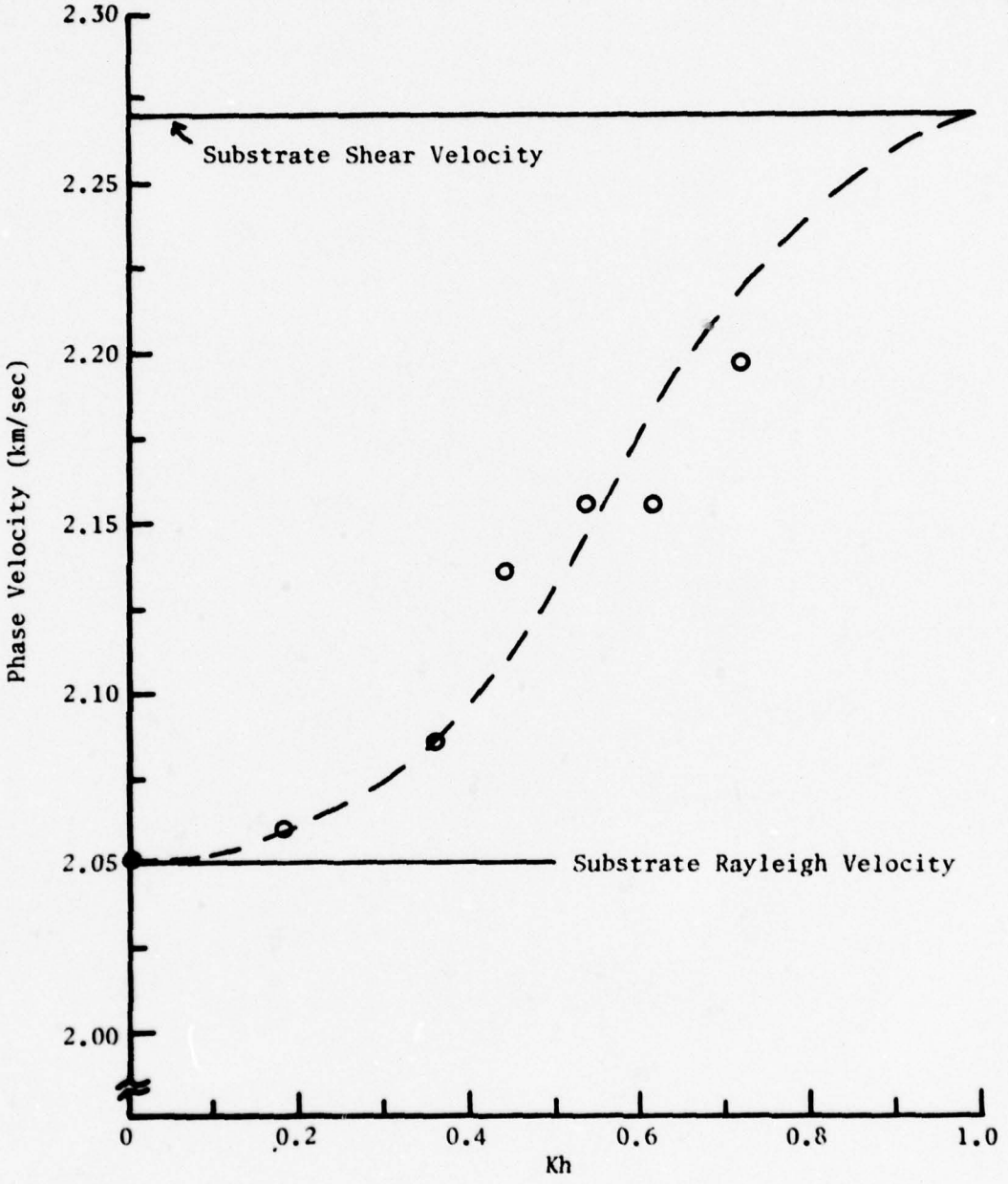

Figure 13. Plot of phase velocity vs. Kh for aluminum on copper ($\hat{V}_S > V_S$) in water.

from that shown for silicon on zinc oxide. Indeed, a point of inflection occurs near Kh = 1/2 when the data are plotted for aluminum on copper. It should be noted however that this sample does not obey the strongly stiffening condition of Farnell and Adler.

The data for aluminum on brass are plotted in Figure 14. The resemblance to Figure 2, page 7, for silicon on zinc oxide is again noticeable, as the phase velocity approaches the substrate shear velocity over a limited range of Kh. However, again the curvature in the region near Kh = 0 is like that for the aluminum on copper sample, and quite different from that evident in Figure 2. The aluminum on brass sample does obey the strongly stiffening condition of Farnell and Adler. It appears that the observed behavior near Kh = 0 may be characteristic in cases of stiffening since it is observed in the plots for both samples.

Other samples. Stiffening was examined using other samples as shown in Table 10. For stainless steel on copper, the layer thickness h is about 10% of the substrate Rayleigh wavelength, and the phase velocity increases by 6% over V_R. The brass substrate and copper layer have nearly the same shear velocity, that of copper being slightly higher. The fact that copper causes an increase in V over V_R indicates that such an increase will occur regardless of the shear velocity differential as long as $\hat{V}_S > V_S$, as the theory predicts in the vacuum-solid layer-solid case.

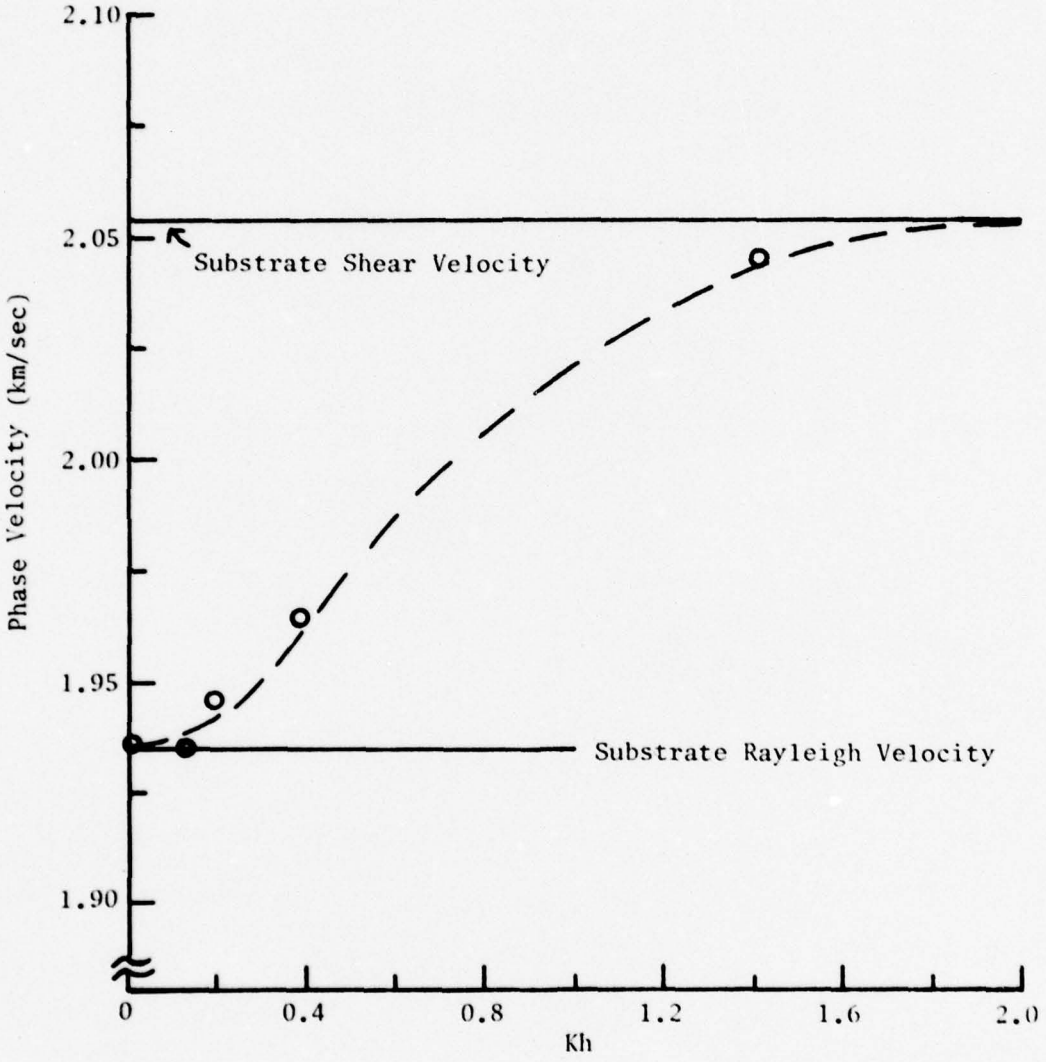

Figure 14. Plot of phase velocity vs. Kh for aluminum on brass ($V_S > V_S$) in water.

TABLE 10

PHASE VELOCITIES CALCULATED FROM THE RAYLEIGH ANGLES MEASURED FOR OTHER "STIFFENED" SAMPLES

Substrate	Layer	h (μ)	f (MHz)	Kh	θ_R	V (m/sec)
Copper	Stainless Steel	0	2	0	46.3°	2050
		102	2	0.63	43.0°	2175
Brass	Stainless Steel	0	2	0	50.0°	1935
		102	2	0.66	47.3°	2015
Brass	Nickel	0	2	0	50.0°	1935
		45	2	0.29	49.5°	1950
		45	5	0.73	48.5°	1980
Brass	Copper	0	2	0	50.0°	1935
		115	2	0.75	48.3°	1985

Lead and Plexiglass as Substrates

Lead and plexiglass have shear velocities lower than the longitudinal velocity of water, and therefore have no Rayleigh angles. When layers are added to them, however, null strips can be detected. Two types of layers, brass and aluminum, were bonded to lead, thus causing null strips to appear at the angles shown in Table 11.

Plexiglass is perhaps a more interesting sample to study. Between 42° and 72° incidence, the reflection coefficient is so small (Smith, 1971) that no reflected beam can be seen. Also, recent experiments (Breazeale, 1978, p. 45) have shown that a null strip can be detected for plexiglass at an angle of 40° even though no Rayleigh angle exists. Layers of brass and stainless steel were bonded onto plexiglass, and the angles at which null strips were observed are given in Table 12. A null strip was observed for the plexiglass at 40°, but the addition of the thin layers causes an increase of about 15° in the angle at which the null strip is seen. The 152μ brass layer, comparable to a thin plate, was examined at 2 MHz to determine whether the 53° null strip might be attributed to a plate mode, but no null strip occurred near that angle for the thin plate. In each case, a reflected beam is present at all angles when a layer is deposited on plexiglass, unlike for the plain substrate.

B. ETHANOL AS THE PROPAGATING MEDIUM

The liquid-solid layer-solid problem was further studied by testing loading and stiffening using ethanol as the liquid medium. The

TABLE 11

THIN LAYERS ON LEAD

Layer	h (μ)	f (MHz)	θ_R	V (m/sec)
Brass	152	2	59.0°	1730
Aluminum	29	3	56.0°	1790

TABLE 12

THIN LAYERS ON PLEXIGLASS

Layer	h (μ)	f (MHz)	θ_R	V (m/sec)
Brass	152	2	53.0°	1855
Steel	25	2	55.0°	1810
	51	2	54.5°	1820
	76	2	54.0°	1830

longitudinal velocity of ethanol was measured to be 1170 m/sec, and the density was taken as 0.79 g/cm^3 from the CRC Handbook of Chemistry and Physics.

Loading ($\hat{V}_S < V_S$)

The 69μ copper layer on stainless steel was examined with three different frequencies to test loading in ethanol. Table 13 shows that as Kh increases, V decreases, and hence the copper-steel sample gives the expected result for loading in ethanol as well as in water. The data are plotted in Figure 15, and as before the curve has been extended to show the data trend for larger Kh values.

Stiffening ($\hat{V}_S > V_S$)

Two substrates were used to test stiffening in ethanol, and the data obtained are given in Table 14. For the copper layer on brass and the steel layers on copper, the phase velocities are larger than the corresponding leaky Rayleigh velocities of the substrates as the theory predicts for the vacuum-solid layer-solid case.

C. ETHANOL-WATER MIXTURE AS THE PROPAGATING MEDIUM

Pure ethanol has a much lower longitudinal velocity than water, but in a mixture of the two containing 25% ethanol by volume, the speed of sound is greater than in either liquid. Such a mixture was used as still another propagating medium to examine the liquid-solid layer-solid

TABLE 13

LOADING IN ETHANOL. PHASE VELOCITIES CALCULATED FROM THE RAYLEIGH ANGLES MEASURED FOR COPPER ON STAINLESS STEEL

h (μ)	f (MHz)	Kh	θ_R	V (m/sec)
0	2	0	26.0°	2670
69	2	0.32	26.7°	2605
69	3	0.49	27.0°	2575
69	6	0.97	28.3°	2470
∞ (calculated)		∞	33.3°	2130

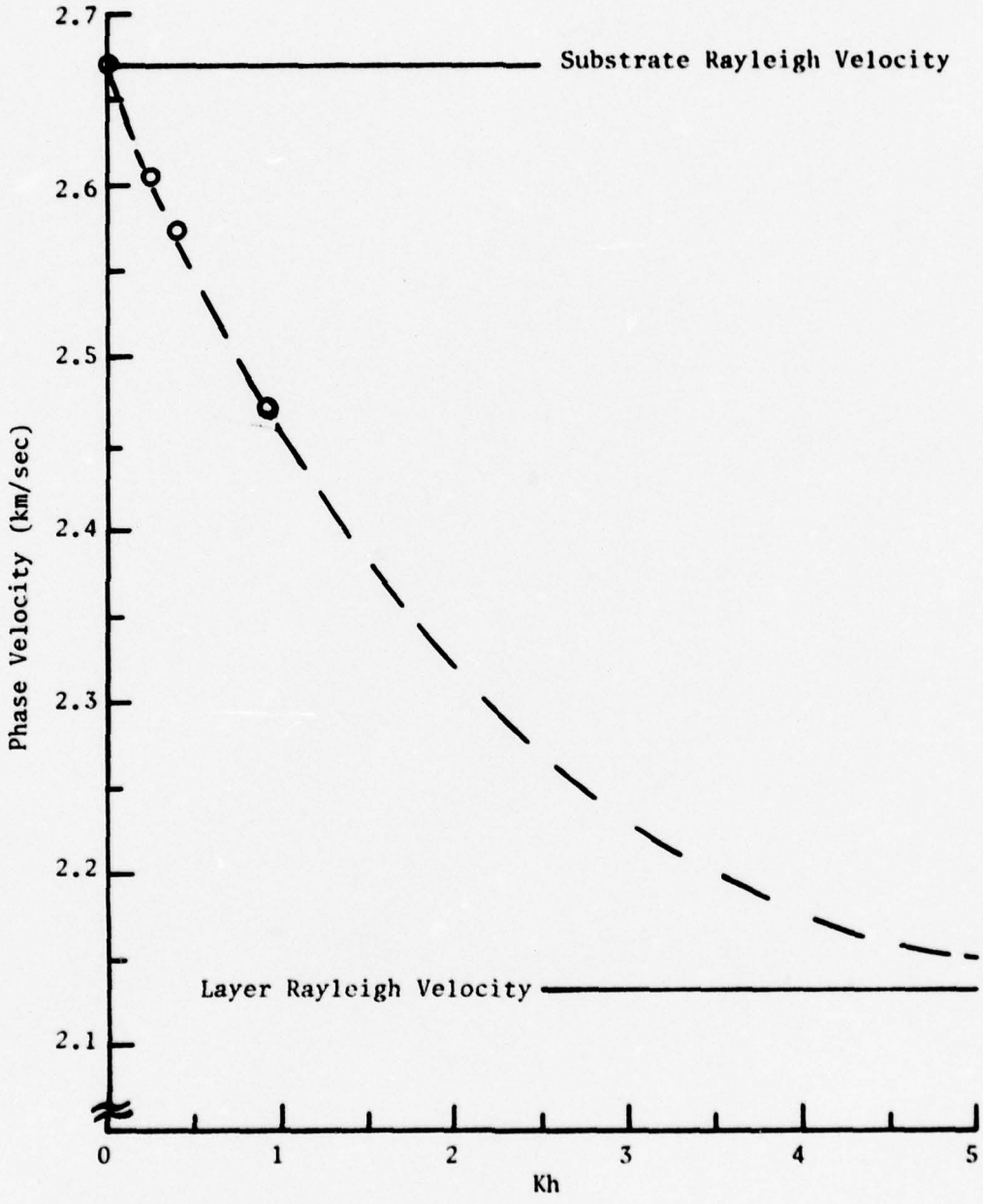

Figure 15. Plot of phase velocity vs. Kh for copper on stainless steel ($V_S < V_S$) in ethanol.

TABLE 14

STIFFENING IN ETHANOL. PHASE VELOCITIES CALCULATED FROM THE RAYLEIGH ANGLES MEASURED FOR SAMPLES STIFFENED IN ETHANOL

Substrate	Layer	h (μ)	f (MHz)	Kh	θ_R	V (m/sec)
Brass	Copper	0	2	0	39.5°	1840
		115	2	0.79	38.5°	1880
Copper	Steel	0	2	0	37.0°	1945
		25	2	0.16	36.5°	1965
		51	2	0.32	36.0°	1990

problem. The longitudinal velocity in the mixture was measured at 1552 m/sec. The density was taken as 0.95 g/cm^3 by averaging the densities of the two component liquids with appropriate weighting factors to account for the fraction of each component present in the mixture. Only a few examples were studied in this liquid due to heat schlieren problems caused by the exothermic mixing process.

Loading ($\hat{V}_S < V_S$)

Copper on steel was again used to test loading. As the data in Table 15 show, $V < V_R$ for each Kh value just as in water and pure ethanol, and as expected from the Farnell-Adler theory.

Stiffening ($\hat{V}_S > V_S$)

In water, aluminum oxide on steel causes the phase velocity to be lower than the steel Rayleigh velocity, although one might expect it to be higher since $\hat{V}_S > V_S$. The data in Table 16 indicate that the behavior observed in water occurs in the mixture as well.

D. COMPARISON OF CALCULATED AND OBSERVED RAYLEIGH VELOCITIES

Equation 2 on page 10, due to Überall (1973), has been used by investigators to calculate the Rayleigh velocity of a material immersed in a liquid medium. This section compares measured values with values calculated from this equation for samples in each of the three liquids previously discussed, whose properties are summarized in Table 17. The properties of the samples are given in Table 1, page 21.

TABLE 15

LOADING IN THE ETHANOL-WATER MIXTURE. PHASE VELOCITIES CALCULATED FROM THE RAYLEIGH ANGLES MEASURED FOR COPPER ON STAINLESS STEEL

h (μ)	f (MHz)	Kh	θ_R	V (m/sec)
0	2	0	34.0°	2775
69	2	0.31	35.5°	2675
69	3	0.47	36.0°	2640
69	5	0.78	37.0°	2580
∞ (calculated)		∞	46.7°	2135

TABLE 16

PHASE VELOCITIES CALCULATED FROM THE RAYLEIGH ANGLES MEASURED FOR ALUMINUM OXIDE ON STAINLESS STEEL IMMERSED IN THE ETHANOL-WATER MIXTURE

h (μ)	f (MHz)	Kh	θ_R	V (m/sec)
0	2	0	34.0°	2775
100	2	0.45	38.0°	2520
100	3	0.68	38.3°	2505
100	5	1.13	40.0°	2415
∞ (calculated)		∞	16.5°	5465

TABLE 17

PROPERTIES OF LIQUID MEDIA

Liquid	ρ (g/cm^3)	V_L (m/sec)
Water	1.0	1482
Ethanol	0.79	1170
Mixture	0.95	1552

Samples Immersed in Water

Table 18 gives the calculated and measured values of the Rayleigh velocity for each of the six samples studied. There is excellent agreement between the observed and calculated values (within 1%) in every case except for the copper, which shows a 4% difference. The pulse-echo technique used in measuring the shear velocity of the copper sample is less accurate than the methods used for the other samples, and as much as a 3% error is conceivable. A shear velocity 3% lower than that listed for copper would give a calculation very close to the observed value.

Samples Immersed in Ethanol

The Überall equation has accurately predicted Rayleigh velocities for materials immersed in water, but the equation must now be tested for other liquids. Table 19 lists results obtained for the same six samples when ethanol is used as the propagating medium. The last column in the table shows the percentage difference between expected and measured Rayleigh velocities, and for each sample the theory and experiment differ by more than can be expected from experimental error. Even for the copper, a 3% error in shear velocity measurement would not cause such deviation.

Samples Immersed in the Ethanol-Water Mixture

Only three samples were studied in the mixture, and results are given in Table 20. The measured Rayleigh velocity for aluminum oxide agrees well with the Überall calculation, but for the stainless steel and copper, the difference is much greater.

TABLE 18

COMPARISON OF CALCULATED AND MEASURED RAYLEIGH VELOCITIES FOR SAMPLES IN WATER

Sample	θ_R		V_R	
	Calculated	Observed	Calculated	Observed
Stainless Steel	30.4°	30.5°	2930	2920
Aluminum	30.6°	31.0°	2910	2875
Brass	50.5°	50.0°	1920	1935
Copper	44.0°	46.3°	2135	2050
Glass	28.6°	28.5°	3095	3105
Aluminum Oxide	15.54°	15.5°	5530	5545

TABLE 19

COMPARISON OF CALCULATED AND MEASURED RAYLEIGH VELOCITIES FOR SAMPLES IN ETHANOL

Sample	θ_R		V_R		Difference
	Calculated	Observed	Calculated	Observed	
Stainless Steel	23.5°	26.0°	2935	2670	9%
Aluminum	23.8°	25.7°	2900	2700	7%
Brass	37.6°	39.5°	1920	1840	4%
Copper	33.3°	37.0°	2135	1945	9%
Glass	22.3°	25.5°	3085	2720	12%
Aluminum Oxide	12.2°	14.0°	5535	4835	13%

TABLE 20

COMPARISON OF CALCULATED AND MEASURED RAYLEIGH VELOCITIES FOR SAMPLES IN THE ETHANOL-WATER MIXTURE

Sample	θ_R		V_R		Difference
	Calculated	Observed	Calculated	Observed	
Stainless Steel	32.0°	34.0°	2930	2775	5%
Copper	46.7°	51.0°	2135	2000	6%
Aluminum Oxide	16.3°	16.5°	5530	5465	1%

CHAPTER V

SUMMARY AND CONCLUSION

The phase velocity of the Rayleigh-like mode in the liquid-solid layer-solid problem behaves in the same manner expected in the vacuum-solid layer-solid case discussed by Farnell and Adler (1972) in all samples studied with two notable exceptions. The zirconium oxide and aluminum oxide layers on stainless steel obey the condition for stiffening since the layer shear velocities exceed the substrate shear velocities (although the zirconium oxide on steel does not obey the Farnell-Adler condition for strong stiffening because $\hat{V}_S < \sqrt{2}\, V_S$). In both cases the phase velocity decreases with increasing Kh, the result expected for loading on the basis of the Farnell-Adler theory.

It is probable that the way these samples were prepared led to this unexpected behavior. As explained on page 20, the ceramic layers under consideration were spray coated onto the stainless steel substrate, the only materials so deposited. The process requires the ceramic to be heated to the melting point and then sprayed onto the steel where it hardens as it cools. This method produces the least smooth layers of all deposition methods used, and in fact the ceramic layers are quite grainy. This is surely a non-negligible condition and could lead to the observed behavior. It is likely that the elastic properties of the ceramic layers were altered by the spray coating process, and as a result the shear velocities of the layers may have been lowered below

that of the steel so that the layers load rather than stiffen the substrate. Shear wave velocities as low as 250 M/sec have been observed in similarly granular sediments [Breazeale and Bjørnø (1977)].

Another important point to consider is the manner in which the curves in Figures 13 and 14, pages 37 and 39, for stiffening approach the substrate Rayleigh velocity in the Kh = 0 region. The theoretical curve of Farnell and Adler for silicon on zinc oxide (Figure 2, page 7) shows a steep slope in this region. Data for aluminum layers on copper and brass in water indicate that there is a minimum layer thickness below which no measurable change in phase velocity occurs. As a result the phase velocity calculated from the data increases with increasing Kh much more slowly near Kh = 0 than suggested by the theory for the vacuum-solid layer-solid case.

CHAPTER VI

SUGGESTIONS FOR FURTHER WORK

The following is a list of ideas which may be developed for completeness:

1. At present, no theory is available to predict the behavior of the phase velocity for the liquid-solid layer-solid problem. It would be desirable to develop a theory describing the problem.

2. Most of the phase velocities reported in this thesis were given for $Kh < 1$. Other investigators might use thicker layers and higher frequencies in order to fill out the curves for phase velocity vs. Kh in more detail.

3. The manner in which the curves approach $Kh = 0$ in the case of stiffening should be further investigated to see if there is indeed a difference between the Farnell-Adler prediction in a vacuum and the observed behavior in a liquid medium.

4. An investigation of the application of the equation cited by Überall must be made in more detail to see how well the equation predicts Rayleigh velocities in other liquid media.

5. No difference was measured in Rayleigh angle between the circular and rectangular electrodes used in this study. However, both types of electrodes produce Gaussian beams. A direct comparison should be made between the rectangular electrodes and the circular electrodes, used by some investigators, which have the same diameter as the transducer but which produce non-Gaussian beams.

6. An expansion of this work could be made by giving a more quantitative measurement of the amplitude in the reflected beam.

7. An obvious extension of this problem would be the study of multilayered media.

BIBLIOGRAPHY

BIBLIOGRAPHY

Adler, Laszlo and D. A. McCathern, "Reflection of a Gaussian Ultrasonic Beam from Al_2O_3 Layer-Stainless Steel in Water at the Rayleigh Angle," J. Appl. Phys. 49:2576 (1978).

Bertoni, H. L. and T. Tamir, "Unified Theory of Rayleigh-Angle Phenomena for for Acoustic Beams at Liquid-Solid Interfaces," Applied Physics, 2:157, 1973.

Breazeale, M. A., "Ultrasonic Wave Reflection at Liquid-Solid Interfaces" (Technical Report 15, Department of Physics, The University of Tennessee), p. 45, 1978.

Breazeale, M. A., Laszlo Adler, and Gerald W. Scott, "Interaction of Ultrasonic Waves Incident at the Rayleigh Angle onto a Liquid-Solid Interface," Journal of Applied Physics, 48:530-537, 1977.

Breazeale, M. A., L. Adler, and J. H. Smith, "Energy Redistribution of a Gaussian Ultrasonic Beam Reflected from a Liquid-Solid Interface," Akusticheski Zhurnal, 21:1, 1975. In Russian.

Breazeale, M. A. and L. Bjørnø, "Forward- and Backward Displacement of Ultrasonic Waves Reflected from a Water-Sediment Interface," Proceedings of Ultrasonics International, Brighton, England, 1977.

Brekhovskikh, L. M., Waves in Layered Media, Academic Press, Inc., New York, 1960.

Ewing, W. M., W. S. Jardetsky, and F. Press, Elastic Waves in Layered Media (McGraw-Hill Book Company, Inc., New York, 1957).

Farnell, G. W. and E. L. Adler, Physical Acoustics, edited by W. P. Mason and R. N. Thurston (Academic, New York, 1972), Vol. IX, pp. 35-127.

Garber, J. W., "Ultrasonic Interactions at Liquid-Solid Boundaries," M.S. Thesis, The University of Tennessee, Knoxville, 1966.

Scott, G. W., "Amplitude and Phase of Rayleigh-Angle Reflections of Gaussian Ultrasonic Beams Incident on Liquid-Solid Interfaces," M.S. Thesis, The University of Tennessee, Knoxville, 1975.

Smith, J. H., "Energy Redistribution in an Ultrasonic Beam Reflected at a Liquid-Solid Interface," M.S. Thesis, The University of Tennessee, Knoxville, 1971.

Smith, R. F., "Lateral Displacement of an Ultrasonic Beam Upon Reflection from a Solid Immersed in a Liquid," M.S. Thesis, The University of Tennessee, Knoxville, 1968.

Überall, H., Physical Acoustics, edited by W. P. Mason and R. N. Thurston (Academic, New York, 1973), Vol. X, pp. 1-57.

Weast, Robert C. (editor-in-chief), Handbook of Chemistry and Physics (CRC Press, Cleveland, Ohio, 54th edition, 1973).

SEPTEMBER 1976

DISTRIBUTION LIST FOR ONR PHYSICS PROGRAM OFFICE
UNCLASSIFIED CONTRACTS

Director Defense Advanced Research Projects Agency Attn: Technical Library 1400 Wilson Blvd. Arlington, Virginia 22209	3 copies
Office of Naval Research Physics Program Office (Code 421) 800 North Quincy Street Arlington, Virginia 22217	3 copies
Office of Naval Research Assistant Chief for Technology (Code 200) 800 North Quincy Street Arlington, Virginia 22217	1 copy
Naval Research Laboratory Department of the Navy Attn: Technical Library Washington, D. C. 20375	3 copies
Office of the Director of Defense Research and Engineering Information Office Library Branch The Pentagon Washington, D. C. 20301	3 copies
U. S. Army Research Office Box CM, Duke Station Durham, North Carolina 27706	2 copies
Defense Documentation Center Cameron Station (TC) Alexandria, Virginia 22314	12 copies
Director, National Bureau of Standards Attn: Technical Library Washington, D. C. 20234	1 copy
Commanding Officer Office of Naval Research Branch Office 536 South Clark Street Chicago, Illinois 60605	3 copies

San Francisco Area Office — 3 copies
Office of Naval Research
760 Market Street, Room 447
San Francisco, California 94102

Office of Naval Research — 6 copies
Code 102 1P (ONR/L)
800 North Quincy Street
Arlington, Virginia 22217

Air Force Office of Scientific Research — 1 copy
Department of the Air Force
Washington, D. C. 22209

Commanding Officer — 3 copies
Office of Naval Research Branch Office
1030 East Green Street
Pasadena, California 91101

Commanding Officer — 3 copies
Office of Naval Research Branch Office
495 Summer Street
Boston, Massachusetts 02210

Director — 1 copy
U. S. Army Engineering Research
and Development Laboratories
Attn: Technical Documents Center
Fort Belvoir, Virginia 22060

ODDR&E Advisory Group on Electron Devices — 3 copies
201 Varick Street
New York, New York 10014

New York Area Office — 1 copy
Office of Naval Research
715 Broadway, 5th Floor
New York, New York 10003

Air Force Weapons Laboratory — 1 copy
Technical Library
Kirtland Air Force Base
Albuquerque, New Mexico 87117

Air Force Avionics Laboratory — 1 copy
Air Force Systems Command
Technical Library
Wright-Patterson Air Force Base
Dayton, Ohio 45433

Lawrence Livermore Laboratory — 1 copy
Attn: Dr. W. F. Krupke
University of California
P. O. Box 808
Livermore, California 94550

Harry Diamond Laboratories — 1 copy
Technical Library
Connecticut Ave. at Van Ness, N. W.
Washington, D. C. 20008

Naval Air Development Center — 1 copy
Attn: Technical Library
Johnsville
Warminster, Pennsylvania 18974

Naval Weapons Center — 1 copy
Technical Library (Code 753)
China Lake, California 93555

Naval Training Equipment Center — 1 copy
Technical Library
Orlando, Florida 32813

Naval Underwater Systems Center — 1 copy
Technical Library
New London, Connecticut 06320

Commandant of the Marine Corps — 1 copy
Scientific Advisor (Code RD-1)
Washington, D. C. 20380

Naval Ordnance Station — 1 copy
Technical Library
Indian Head, Maryland 20640

Naval Postgraduate School — 1 copy
Technical Library (Code 0212)
Monterey, California 93940

Naval Missile Center — 1 copy
Technical Library (Code 5632.2)
Point Mugu, California 93010

Naval Ordnance Station — 1 copy
Technical Library
Louisville, Kentucky 40214

Commanding Officer — 1 copy
Ocean Research & Development Activity
National Space Technology Laboratories
Bay St. Louis, Mississippi 39520

Naval Explosive Ordnance Disposal Facility — 1 copy
Technical Library
Indian Head, Maryland 20640

Naval Electronics Laboratory Center — 1 copy
Technical Library
San Diego, California 92152

Naval Undersea Center — 1 copy
Technical Library
San Diego, California 92132

Naval Surface Weapons Center — 1 copy
Technical Library
Dahlgren, Virginia 22448

Naval Ship Research and Development Center — 1 copy
Central Library (Code L42 and L43)
Bethesda, Maryland 20084

Naval Surface Weapons Center — 1 copy
Technical Library
Silver Spring, Maryland 20910

Naval Avionics Facility — 1 copy
Technical Library
Indianapolis, Indiana 46218

Dr. Werner G. Neubauer — 1 copy
Code 8130
Physical Acoustics Branch
Naval Research Laboratory
Washington, D.C. 20375

Dr. Bill D. Cook — 1 copy
Dept. of Mechanical Engineering
University of Houston
Houston, Texas 77004

Dr. Floyd Dunn — 1 copy
Biophysical Research Laboratory
University of Illinois
Urbana, Illinois 61801

Dr. E. F. Carome — 1 copy
Department of Physics
John Carroll University
University Heights
Cleveland, Ohio 44017